

# Radiation Hardened RF Transceiver For In-Containment Environment Applications Using Commercial Off the Shelf Components

Shawn C. Stafford<sup>1</sup>, Jorge V. Carvajal<sup>1</sup>, Jonathan E. Baisch<sup>1</sup>

<sup>1</sup>Westinghouse Electric Company

Westinghouse Electric Company, LLC, Global Technology Development, Pittsburgh, PA 15235, USA  
staffosc@westinghouse.com; carvajjv@westinghouse.com; baischje@westinghouse.com

## ABSTRACT

The ability to use wireless devices and other electronics in a radiation environment such as Nuclear Power Plant containment is mostly limited by the radiation sensitivity of these electronics. The benefits derived from wireless technology such as the reduction of the amount of cable needed for new sensors, the reduction of the labor associated with cable routing and the reduction or elimination of containment penetrations for new sensors is significant and well understood; unfortunately these benefits have not been fully accomplished yet because of numerous challenges, one being the radiation environment.

Functional operation and radiation effects of a transceiver, which utilizes an integrated circuit system-on-chip, with a micro controller, serial driver, phase-locked loop, crystal oscillators and an RF amplifier, will be described. The second type of transceiver that will be discussed uses discrete components such as JFETs, MOSFETs and op-amps to perform the signal conditioning and RF transmission is also described. Operation capabilities and radiation effects for these two approaches as well as energy sources will be described and compared in detail.

*Key Words:* wireless, gamma radiation, nuclear power plant.

## 1 INTRODUCTION

Today's integrated circuits provide an enormous level of flexibility in terms of functional capabilities, small footprint, low power consumption and relatively inexpensive cost. Point to point, mesh or star configured wireless nodes are common place in many industrial applications [1]. From a functional perspective, these types of commercial-off-the-shelf (COTS) options would be acceptable in a Nuclear Power Plant (NPP). The major problem for a NPP primary side application or post-accident conditions becomes the environment, most notably the radiation environment [2].

The first type of wireless transmitter/receiver that will be discussed uses a System on Chip (SoC) integrated circuit (IC) as the main processing means and radio frequency (RF) section. This type of approach as stated previously provides a low power consumption and small footprint option with the ability to transmit an encrypted spread spectrum signal. The second type of wireless transmitter/receiver approach uses discrete components such as JFETs, MOSFETs, inverters, flip-flops and timer modules. These components were selected because they are the essential building block of any transmitter and receiver. The following sections will break down each of the main components of each approach and describe the irradiation test results.

## 2 SCOPE

### 2.1 Microcontroller Based Wireless Transmitter

The equipment under test (EUT) is listed below:

- Transmitter prototype board with signal conditioning circuit.
- Receiver prototype board.
- One Lithium Thionyl-Chloride 3.6 V, 7.7 A-hour battery.
- One Lithium Thionyl-Chloride 3.6 V, 16.5 A-hour battery.

The transmitter and receiver boards contain a Radio Frequency (RF) Integrated Circuit (IC) transceiver, a current to voltage signal conditioning front end, analog to digital converter (ADC) and supporting circuitry such as two crystals oscillators (reference clocks), voltage regulator, an SMA connector, resistors, inductors and capacitors.

#### 2.1.1 Transmitter Board

Figure 1 shows the transmitter board that was tested inside the Clean Hot Cell (CHC). As shown in the figure, the AAA batteries were not installed and instead an external power supply was used to power the board. An RF cable is connected to the SMA test point, which is used to monitor the amplitude output. The SMA test point is a high isolation coupled output from the main RF output. The input signal is connected to header J12 as shown on the left hand side of the figure.

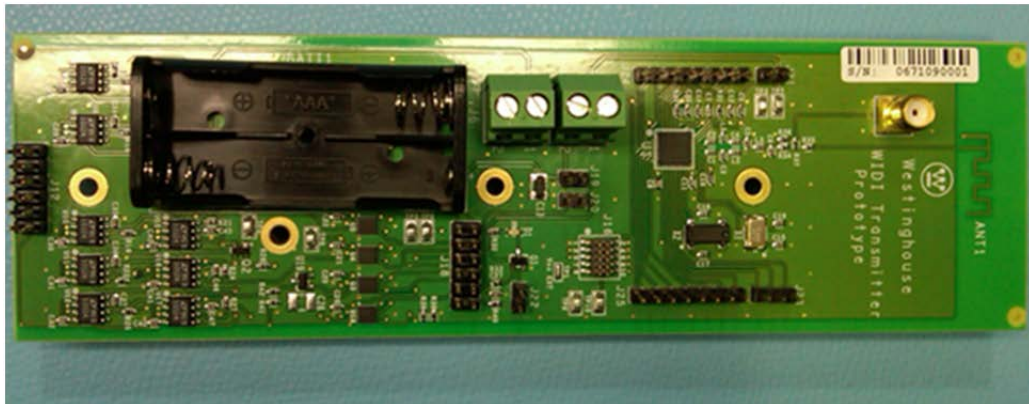


Figure 1. Transmitter board with RF IC.

#### 2.1.2 Receiver Board

Figure 2 shows the receiver board that was tested inside the CHC. The board was also powered externally though the J9 connector shown on the upper left side of Figure 2. An RF cable is connected to the SMA test point similarly to the transmitter board. The data received is recorded through the RS-232, J1 connector shown on the lower left side.



Figure 2. Receiver board with RF IC.

### 2.1.3 Batteries

Two high density D cell Lithium Thionyl-Chloride batteries were connected to a load resistor in order to draw a current representative of the transmitter board current draw during normal operation. The resistors were located outside of the hot cell. The batteries under test were placed in a polycarbonate enclosure as a safety precaution in case of an explosion due to the potential radiation induced short circuit. Each battery was set up to draw 22mA.

## 2.2 Discrete Component Based Transmitter/Receiver Board

The equipment under test (EUT) is listed below:

**Table I. Type of functions and components**

Function	Component
Op Amp/BJT Current Sources	Op Amp & BJT
Clock Oscillator and Dividers	HCMOS clock oscillator, flip-flop and decade counter
Transistor Amplifiers	JFET and MOSFET
Power supply	Linear voltage regulator
RF Oscillator	Crystal oscillator and JFET
Low Frequency Oscillator	HCMOS and JFET
RF Receiver	Integrated IC

Op Amp/BJT Current Sources: A general purpose op amp and common bipolar junction transistor (BJT) were configured in a voltage follower transistor driven output to create a current source which delivered 250 uA of current through a load resistor. The voltage developed on the load resistor was monitored externally to the unit. Four identical circuits were in place to increase the statistical sample.

Clock Oscillator and Dividers: A circuit consisting of HCMOS technology was in place to monitor effects of the radiation on a common logic family. The circuit contained an HCMOS clock oscillator module driving an HCMOS flip-flop IC and two HCMOS decade counters. The outputs of these circuits were 10 kHz clock signals. There were 2 of these circuits in place to increase the statistical sample.

Transistor Amplifiers: Eight transistor amplifier circuits were included to determine effects of radiation on common amplifier configurations using two kinds of transistors: JFET's and MOSFET's. The amplifiers were configured as common source amplifiers and biased for class A operation. The JFET's are a common depletion mode N channel device and were self-biased to provide gain. The MOSFET's are common enhancement mode N channel FET's and were also biased to provide gain.

Power Supply: A DC power supply was realized with half wave rectification and regulation to provide the power for the entire unit. The rail voltages were developed using common linear regulators which provided + 15VDC, - 15 VDC, and +5 VDC. Although these outputs were not directly monitored, failures of the supply would be evident in the coincident failure of several circuits in the unit.

Radio Frequency (RF) Oscillator: Two RF crystal oscillators were included to determine the effects of the radiation on signal sources. A common JFET transistor was the only active element in the oscillator; no output amplifiers or buffers were used. Commonly available crystals (20 MHz, and 20.5 MHz) were used to control the frequency output.

Low Frequency Oscillator: Another HCMOS circuit was included to produce a low frequency signal (approx. 100 Hz) which was used to amplitude modulate each JFET RF oscillator. The oscillator was realized using a common un-buffered inverter gate IC configured as an RC square wave oscillator.

RF Receiver: A highly integrated wideband FM receiver integrated circuit was used to receive the signal from the JFET and detect the modulated signal imposed on the RF oscillator by the low frequency gate oscillator. Although an FM receiver IC was used, the AM signal was detected on the “squelch” output of the receiver derived from the internal limiter action of the IC, where an output current was developed dependent on the incoming signal strength. This signal was then amplified and detected using a comparator comprised of another common op amp to develop a logic level signal relating to the original low frequency modulating signal. The receiver IC consists of an RF front end amplifier, RF mixer, limiter and quadrature detection circuit. Since the data output signal is derived from the, the quadrature circuit was not involved in the receiver function. However an internal data comparator is included in the IC which was used to develop the 5 V logic level output from the previous op amp amplifier/comparator stage.

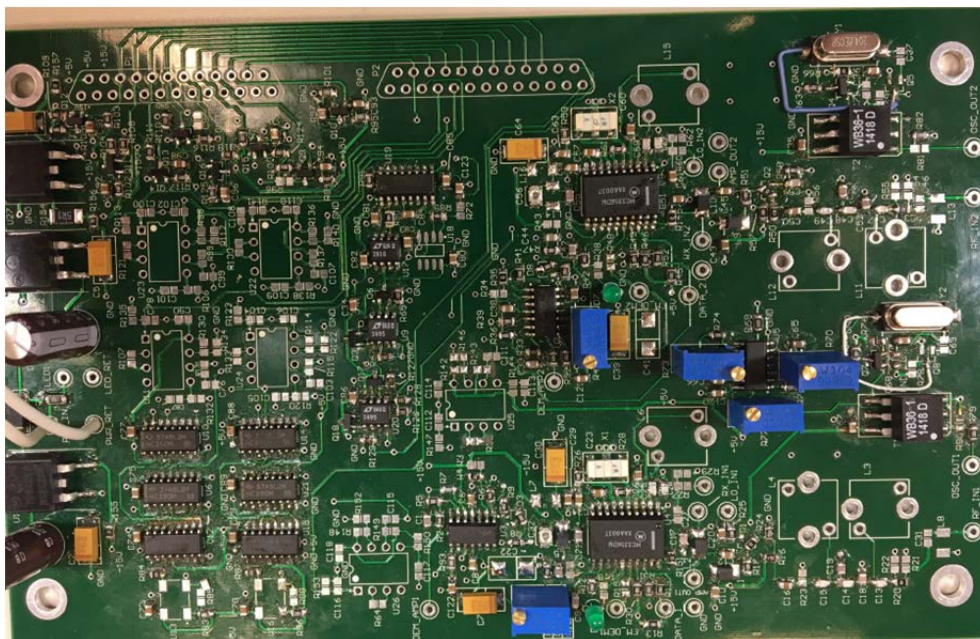


Figure 3. Transmitter & Receiver board with discrete components.

### 3 TEST SETUP

#### 3.1 Microcontroller Based Wireless Transmitter/Receiver CHC Test Configuration

Figure 4 depicts the high level schematic of the microcontroller based board. There are two op-amp stages that are used to convert a current signal into a suitable voltage for the analog-to-digital converter (ADC). The ADC then sends a serial stream of data to the SoC RF Transceiver. The RF transmitter was setup in continuous mode to transmit a 2.4GHz signal at 0dBm.

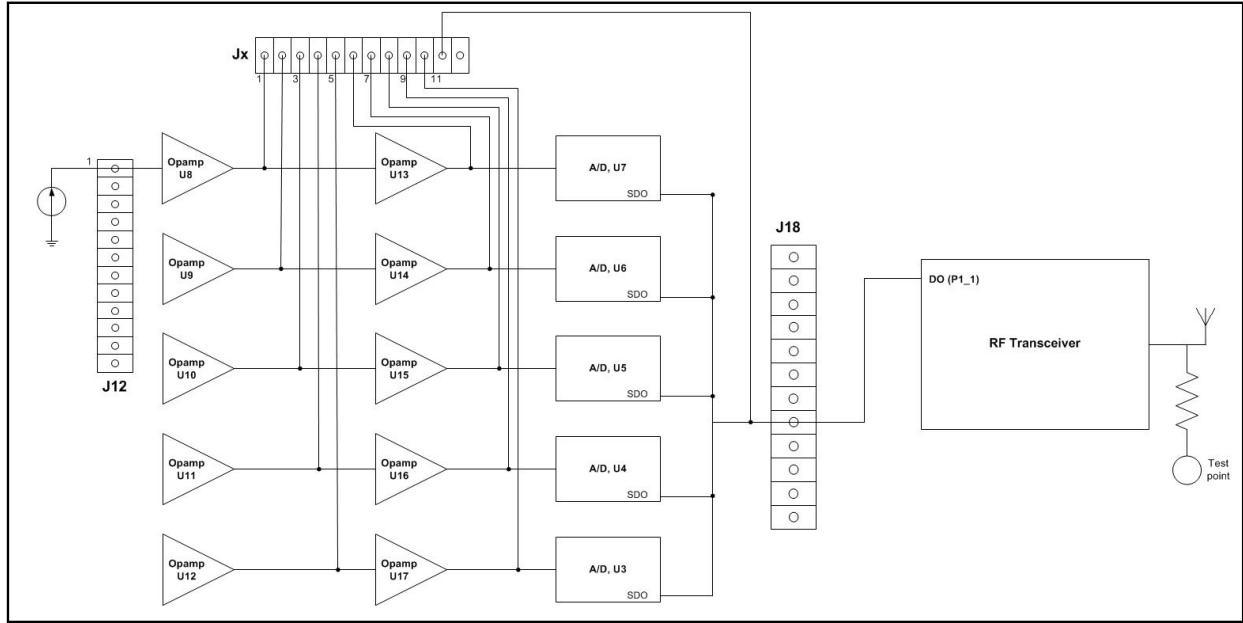


Figure 4. Micro controller based wireless transmitter and battery test setup

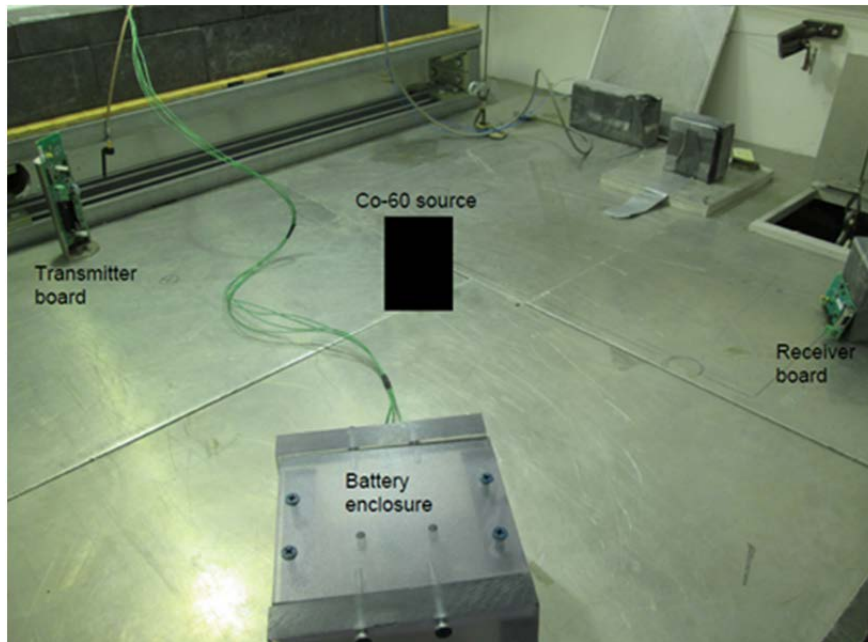
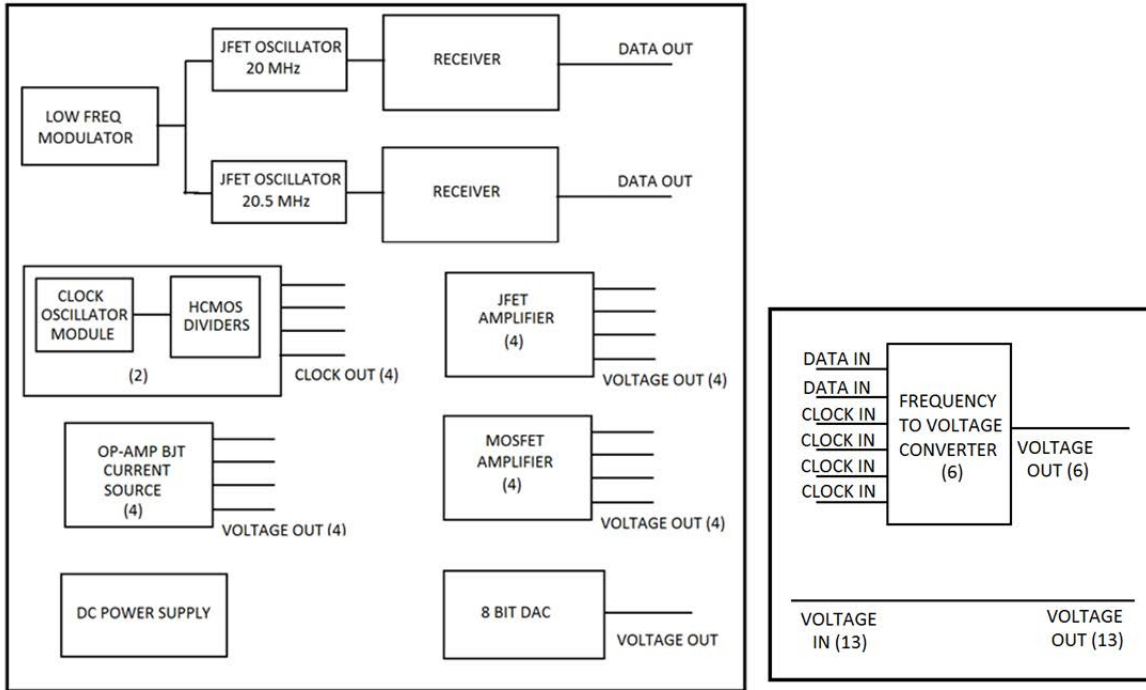


Figure 5. Clean Hot Cell test setup for Micro controller based wireless transmitter and battery.

### 3.2 Discrete Components Transmitter/Receiver Hot Cell Test Configuration

Figure 6 shows on the left side the type of components assembled on the board that were irradiated and on the right hand side a board used as a signal conditioner for the National Instrument monitoring hardware.





**Figure 6. Discrete Components high level schematic tested in CHC (left) and interface board outside CHC (right).**

Figure 7 shows the board setup within the hot cell. In order to achieve the dose required of approximately 1 Mrad, the Co-60 source had to be placed relatively close to the board.



**Figure 7. Clean Hot Cell Test Setup for Discrete Components board. Co-60 source indicated by inset box.**

## 4 TEST RESULTS

### 4.1 Microcontroller Based Wireless Transmitter/Receiver & Battery Irradiation Results

#### 4.1.1 Batteries

Two 3.6V high density D cell Lithium Thionyl-Chloride batteries were connected to a load resistor in order to draw 22mA of current, which is representative of the integrated low power consumption transmitter board during normal operation.

Battery PN LS26500, with a capacity of 7.7 A-hr, survived 104 krad after approximately 258 hours, while a different battery of the same characteristics lasted 452 hours. It is obvious that the exposure to gamma radiation significantly decreased its capacity.

Battery PN TL-2300, with a capacity of 16.5 A-hr has received 304 krad at its voltage is still holding constant at 3.6V.

#### 4.1.2 Microcontroller Based Transmitter Op-amps

The two op-amps shown in Figure 8 in addition to U12 and U17 from Figure 4 were exposed to 183 krad, without any change to their output voltage performance. The test was stopped on these op-amps prior to any performance degradation was detected.

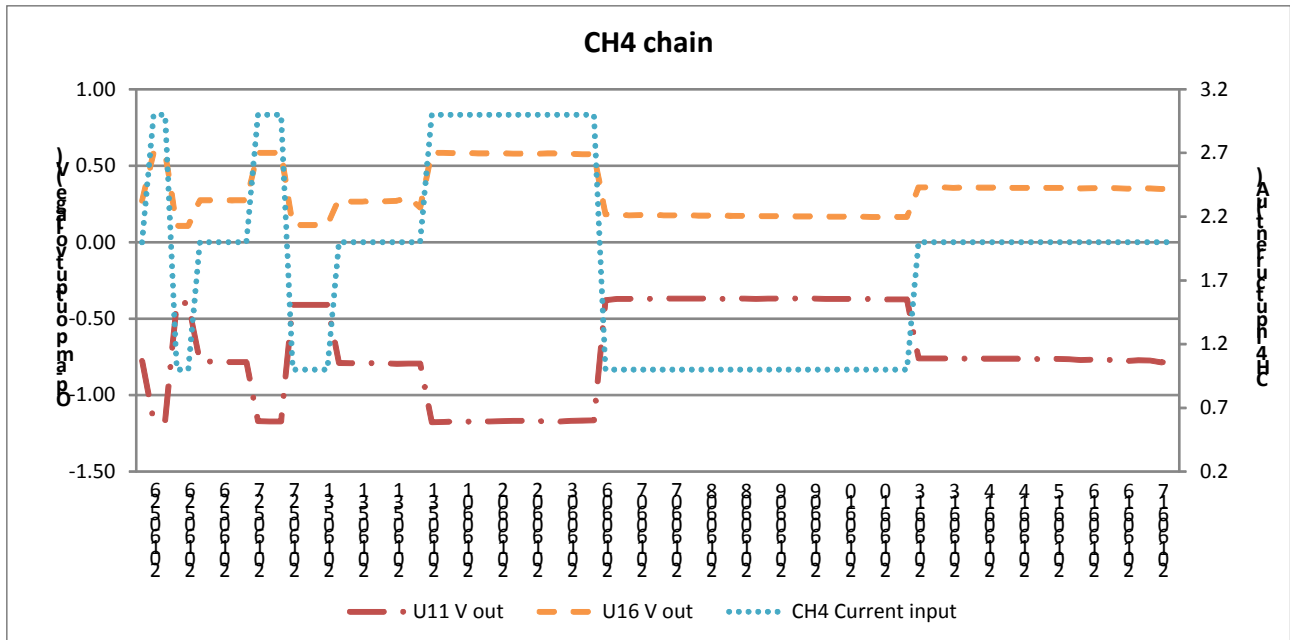


Figure 8. Op-amp U11 and U16 voltage output

#### 4.1.3 Transmitter and Receiver Serial Data

The wireless transmission from the transmitter board was monitored by extracting the digital data through the Universal Asynchronous Receiver/Transmitter (UART) port and by the Spectrum Analyzer connected to the SMA test point connector. The data received wirelessly by the receiver board was also extracted through the UART port. Each transmitted data package was recorded by the data acquisition software every 1 second for the transmitter and receiver board. Figures 9 shows the transmitted (Tx) and received (Rx) signal tracking each other as the input changes for approximately 6 hours. The

microcontroller portion that controls the UART communications started to degrade approximately at 46 krads as shown in Figure 9.

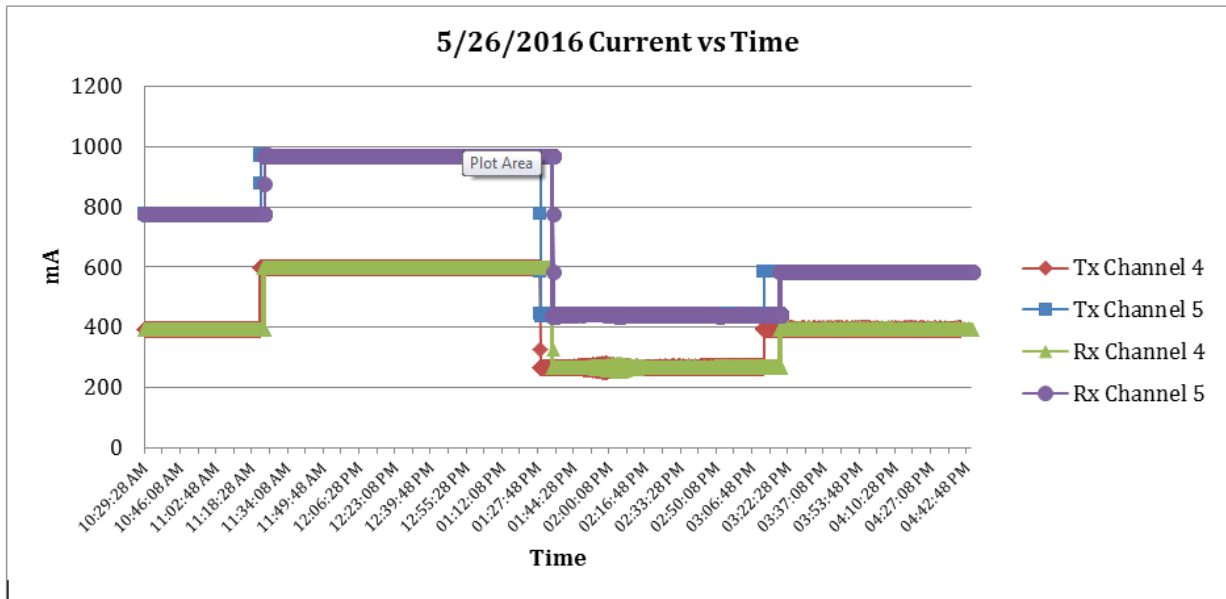


Figure 9. RF Transmitter and Receiver Serial Data

#### 4.2 Discrete Component Based Transmitter/Receiver Board Irradiation Results

Some discrete component circuits showed immediate effects of exposure to the radiation. See Figure 10 below. The MOSFET amplifier bias conditions were immediately affected with a nearly linear consistent decrease in bias voltage. At approximately 22 krads the decrease ended when the Co-60 sources were removed to make alterations to the setup. Early into the test, the DAC output voltage dropped to approximately – 11 VDC. The RF receiver data shows an increase in voltage which corresponds to an increase in the output frequency, likely due to extraneous pulses which when processed by the frequency to voltage converters leads to an increase in output voltage. Other circuits such as the JFET amplifiers, HCMOS clock oscillators and dividers, and the BJT/Op-Amp current sources show no signs of change.

Longer term exposure shows various effects on all circuits in the unit as shown in Figure 11. In this plot some of the redundant circuit outputs were removed to improve clarity since similar circuit types behaved in the same manner. At approximately 150 krads all circuits show signs of degradation or failure. At approximately 1.05 Mrads all circuits show a coincident failure which remained except for a resurgence of circuit activity starting after 1.2 Mrads, although proper circuit functions did not return, after which the total circuit failure returned and remained for the duration of the exposure.

Following the exposure the unit was removed and circuit failures were analyzed. All power supply rail voltages (+ 15 V, – 15 V and +5 V) were affected. The – 15 V rail voltage was at approximately – 16.5 V while the +15 V and + 5 V outputs were near 0 V. Replacing the + 15 V regulator showed the + 5 V output to be approximately 4.5 V. After replacing all three regulators, many of the unit’s circuit functions were restored to conditions close to those before radiation. Table 1 compares output voltages taken before the unit was exposed to voltages measured after replacing the three voltage regulators. The MOSFET amplifier bias voltage decline that was evident during the exposure appears to be permanent, and the DAC failure also matches the failure seen during the exposure. All other circuits, including the RF receiver circuits, functioned identically to the original pre-radiation operation.



More detailed analysis of the circuits showed no degradation in output voltage swing in the HCMOS clock and logic outputs. Nor was any degradation seen in output voltage swings in op amp based amplifiers, comparators, current sources, or the RF receivers. Measurements made within the DAC circuit show that a separate precision reference IC used to provide the reference voltage was still operating but the output voltage was low by approximately 5%, which is 2 orders of magnitude larger than that specified by the manufacturer.

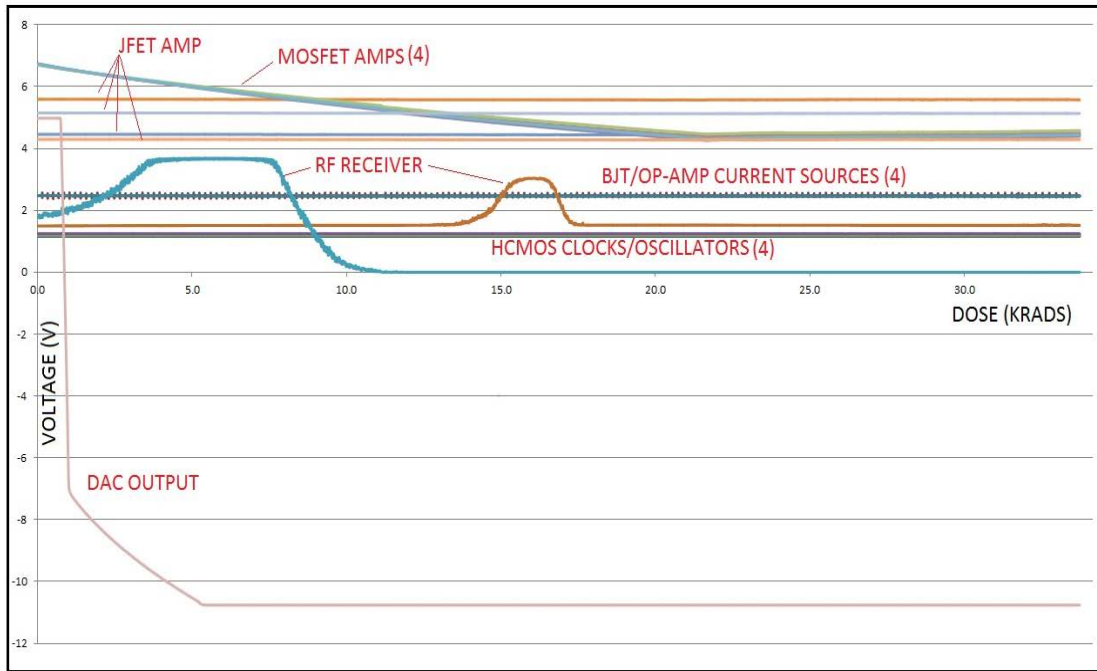


Figure 10. Initial gamma radiation effects of discrete circuit sections

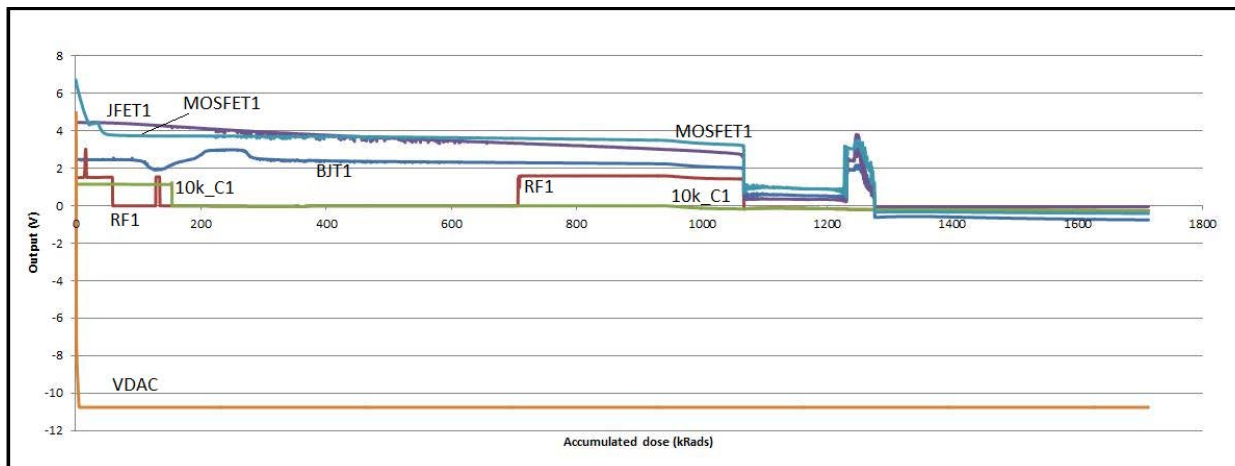


Figure 11. Output voltage variation vs. gamma radiation.

## 5 CONCLUSIONS

An inexpensive low power consumption microcontroller based SoC transceiver board was irradiated and the performance of the signal conditioning op-amps and the SoC was monitored. As expected even COTS type op-amps did not exhibit signs of degradation near 180 krad. The SoC as expected was much more sensitive to the radiation field. The SoC stopped operating around 46 krad, which was observed by UART serial data stream corrupted data. However, the RF portion of the SoC continued to operate until approximately 54 krad. The RF portion output was monitored by a spectrum analyzer connected to the SMA test point. Two types of high density batteries that could power a SoC based board as the one discussed in this paper were also tested and one battery (of two) of one particular type was shown to be significantly affected by the radiation.

A very different alternative to the microcontroller based transceiver was tested in the second part of this research. The types of components selected are the essential building blocks for any transmitter and receiver. The discrete circuits most affected by radiation contained MOSFET components, DAC's, voltage regulators and voltage references. Linear voltage regulators contain an internal reference which is likely the portion of the regulator that was affected, thereby affecting the output voltage. Post exposure analysis of the circuit failures showed that many of the circuit sections were not degraded by the radiation beyond 1 Mrad dose. A single point failure of the power supply caused all circuit sections to fail slightly over 1 Mrad, and faulty power supply operation up to this dose likely caused circuit malfunctions throughout the experiment given that post radiation analysis showed most circuits were fully operational. The circuits received additional dose up to approximately 1.7 Mrad but the circuits were not adequately powered after approximately 1.05 Mrad. If the unit were powered externally it is likely the experiment would have continued well beyond 1 Mrad before showing a board-wide failure.

The project team intends to continue this work and design a hybrid approach, which incorporates some type of shielded microcontroller, radiation hardened discrete components and the off the shelf inherently radiation tolerant components.

## 6 ACKNOWLEDGMENTS

The authors would like to thank the Westinghouse Electric Company Innovation Program for sponsoring the work.

## 7 REFERENCES

1. R. Shankar, Automation in Power Plants and Wireless Technology Assessments, EPRI-1010468, p. 3-4 of Section 3, 2005.
2. E. Guizzo, "Can Japan send in robots to fix troubled nuclear reactors," IEEE Spectrum (2011).